Slow Feature Analysis for Mitotic Event Recognition

Jinghui Chu[1], Hailan Liang[1], Zheng Tong[1], and Wei Lu[1]
[1] School of Electronic Information Engineering, Tianjin University
Tianjin 300072, Tianjin - P. R. China
[e-mail: cjh@tju.edu.cn; lianghailan_2010@sina.com; tongzheng2010@126.com; luwei@tju.edu.cn]
*Corresponding author: Wei Lu

Received August 9, 2016; revised December 1, 2016; accepted January 2, 2017; published March 31, 2017

Abstract

Mitotic event recognition is a crucial and challenging task in biomedical applications. In this paper, we introduce the slow feature analysis and propose a fully-automated mitotic event recognition method for cell populations imaged with time-lapse phase contrast microscopy. The method includes three steps. First, a candidate sequence extraction method is utilized to exclude most of the sequences not containing mitosis. Next, slow feature is learned from the candidate sequences using slow feature analysis. Finally, a hidden conditional random field (HCRF) model is applied for the classification of the sequences. We use a supervised SFA learning strategy to learn the slow feature function because the strategy brings image content and discriminative information together to get a better encoding. Besides, the HCRF model is more suitable to describe the temporal structure of image sequences than nonsequential SVM approaches. In our experiment, the proposed recognition method achieved 0.93 area under curve (AUC) and 91% accuracy on a very challenging phase contrast microscopy dataset named C2C12.

Keywords: Slow feature analysis, mitotic event recognition, hidden conditional random field

This research was supported by the National Natural Science Foundation of China (61271069).

https://doi.org/10.3837/tiis.2017.03.023 **ISSN : 1976-7277**

1. Introduction

Research of stem cell population behaviors has attracted increasing attention in a large range of biomedical applications, such as basic biological research, tissue engineering, and cancer diagnosis. Among all measurements of proliferative behaviors, the accurate detection and localization of mitosis cell benefit all of these biomedical applications as the very first step of research.

For short-duration, small-scale studies, researchers tend to manually label mitosis cells because the visual appearance of mitosis process is easy to be identified as interphase, start of mitosis, formation of daughter cells or separation of daughter cells. However, in a long-duration and high-throughput research, an automated image analysis system is vital.

There are already several working mitotic event recognition approaches for microscopy image sequences. In [1], Li et al. applied a fast cascaded classifier framework to classify volumetric sliding windows based on 3D Haar-like features. In [2], the scale invariance feature transform (SIFT) feature is extracted from candidate patch sequences and fed into an event detection conditional random field (EDCRF) classifier. In [3], Liu et al. proposed a semi-Markov model trained in a max-margin learning framework for mitosis event segmentation. In summary, a typical mitotic event recognition approach generally consists of three phases: candidate extraction, feature extraction, and mitosis classification.

There are several features which represent the characteristics of phase-contrast microscopy images, such as SIFT [4], GIST [5], etc. Inspired by the temporal slowness principle, Wiskott and Sejnowski proposed a nonlinear unsupervised algorithm, namely slow feature analysis (SFA), to extract the stable and slowly varying features from a slice of vectorial input signals [6]. As for the mitosis phase-contrast microscopy images, the importance of generating invariant representations results from two facts: 1) normal cells undergo complex processes including cell division, migration, and drastic variation in morphology; 2) image background suffers from artifacts and changing of illumination.

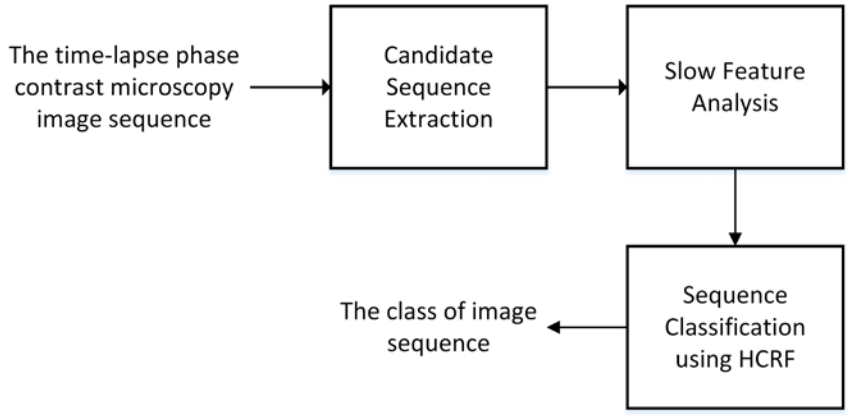

Fig. 1. The SFA-based mitosis detection approach

In this paper, we introduce the slow feature analysis and propose a thorough framework for the task of mitotic event recognition. The framework takes phase contrast microscopy image sequences as input, and automatically outputs localized subregions in the sequences where mitosis occurred. As shown in **Fig. 1**, we first utilize a candidate sequence extraction method

proposed by Liu et al. in [3] to exclude most of the sequences not containing mitosis while keeping all the sequences containing mitosis. Next, we learn the slow feature from candidate sequences using slow feature analysis. Finally, we apply a hidden conditional random field (HCRF) model for the classification of the sequences. We present the technical details of each step in the subsequent sections, with emphasis on the second step.

2. Candidate Sequence Extraction

The goal of candidate sequence extraction is to extract the spatiotemporal subregion sequences that potentially contain mitoses from the original image sequences. In this step, potential mitotic events should be extracted as completely as possible, because any missed mitosis is impossible to recover in the following steps. **Fig. 2** shows two candidate sequences that were automatically extracted by our method. Through this step, the mitotic events are spatially localized and the searching space is effectively reduced from the entire image sequences to the spatiotemporal subregion sequences. Candidate sequence extraction comprises two substeps: 1) image segmentation; 2) spatiotemporal subregion extraction.

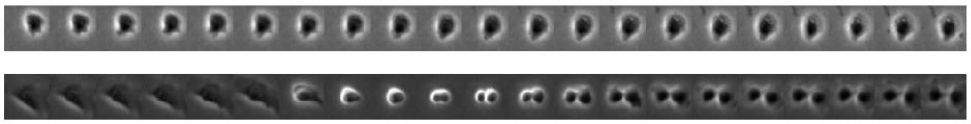

Fig. 2. Negative (top) and positive (bottom) candidate sequences

2.1 Image Segmentation

In this paper, we apply the nonnegative mixed-norm algorithm proposed by Li et al. in [7] to the segmentation of time-lapse phase contrast microscopy image. The time-lapse phase contrast microscopy image can be decently approximated by a linear imaging model, given by

$$\boldsymbol{g} = \boldsymbol{H}\boldsymbol{f} + \boldsymbol{b} + \boldsymbol{n}. \tag{1}$$

Here $\boldsymbol{g}$ denotes a N-dimensional vector representation of the observed image, which is formed by concatenating the image pixels in raster order. The vectors $\boldsymbol{f}, \boldsymbol{b}, \boldsymbol{n}$ represent the ideal object image, bias, and noise respectively. $\boldsymbol{H}$ denotes a $N \times N$ transfer matrix. The linear imaging model is adequate for representing the image formation process of time-lapse phase contrast microscopy.

Given an observed image $\boldsymbol{g}$, we need to compute the ideal object image $\boldsymbol{f}$ with the linear imaging model specified in (1). We solve this inverse problem through a two-step process proposed by Li et al. in [7]. First, we estimate and subsequently eliminate the bias from an observed image. Second, we reconstruct the ideal object image $\boldsymbol{f}$ from the bias-corrected image by minimizing a constrained mix-norm objective function via convex optimization. The mitosis-only image sequences are obtained by solving a linear inverse problem. We refer the interested readers to [7] for more details of the algorithm.

2.2 Spatiotemporal Subregion Extraction

With the mitosis-only image sequences obtained from all input frames, we apply a 3D seeded region growing algorithm in [8] to the image sequences to extract spatiotemporal subregion sequences that potentially contain mitotic events. The algorithm relies on two automatically computed thresholds: a seeding threshold computed by Otsu's method in [9] is used to detect seeds of mitotic regions, and a lower threshold determined by the unimodal thresholding algorithm in [10] is used as the stopping criterion of region growing.

After the two substeps, the candidate sequence is obtained with the size of $h \times w \times d$ ($25 \times 25 \times 21$ in this paper) centered at the selected position (x, y, t), where t denotes the frame index and d denotes the number of frames (as shown in **Fig. 2**). After the candidate sequence is obtained, we apply the image intensity and GIST feature [5] to represent the candidate sequences separately. The image intensity sequence has the size of $h \times w \times d$ ($25 \times 25 \times 21$ in this paper). The GIST feature sequence has the size of $n \times d$ (180×21 in this paper), where n denotes the number of dimensions of GIST feature in each frame.

3. Slow Feature Analysis

3.1 Algorithm

In order to identify the slowest varying feature from the vectorial input signal, SFA solves the following optimization problem. Given an *I*-dimensional input signal $\mathrm{x}(t) = [x_1(t), ..., x_I(t)]^T$, where $t \in [t_0, t_1]$ indicates the time range, SFA works out an input-output function $\mathrm{g}(t) = [g_1(t), ..., g_K(t)]^T$ which makes the *K*-dimensional output signal $\mathrm{y}(t) = [y_1(t), ..., y_K(t)]^T$ with $y_k(t) = g_k(x(t))$ varying as slowly as possible.

The SFA algorithm used in this paper has the following substeps (also shown in **Fig. 3**).

1) *Input signal normalization*: The input signal $\tilde{\mathrm{x}}(t)$ is the candidate sequence which is computed in the previous section. Normalize the input signal to obtain

$$\mathrm{x}(t) := [x_1(t), ..., x_I(t)]^T, \tag{2}$$

where $x_i(t) := (\tilde{x}_i(t) - < \tilde{x}_i >) / \sqrt{< (\tilde{x}_i(t) - < \tilde{x}_i >)^2 >}$, so that $< \tilde{x}_i >= 0$ and $< \tilde{x}_i^2 >= 0$.

2) *Nonlinear expansion*: First, we apply a set of nonlinear functions $\tilde{\mathrm{h}}(\mathrm{x})$ to generate an expanded signal $\tilde{\mathrm{z}}(t)$. For the quadratic SFA (SFA^2), all monomials of degree one and two, including the mixed terms like $x_1 x_2$, are used. Thus, $\tilde{\mathrm{h}}(\mathrm{x})$ and $\tilde{\mathrm{z}}(t)$ are defined as

$$\tilde{\mathrm{h}}(\mathrm{x}) := [x_1, ..., x_I, x_1 x_1, x_1 x_2, ..., x_I x_I]^T, \tag{3}$$

$$\tilde{\mathrm{z}}(t) := \tilde{\mathrm{h}}(\mathrm{x}(t)), \tag{4}$$

where $\tilde{\mathrm{z}}(t)$ and $\tilde{\mathrm{h}}(\mathrm{x})$ have $I + I(I+1)/2$ dimensions.

Then, we normalize the expanded signal $\tilde{\mathrm{z}}(t)$ by an affine transform to generate $\mathrm{z}(t)$ which has a zero mean and identity covariance matrix $\boldsymbol{I}$. Thus, $\mathrm{z}(t)$ are defined as

$$z(t) := \boldsymbol{S}(\tilde{z}(t) - < \tilde{z} >), \tag{5}$$

where $< \tilde{z} >= 0$, $< zz^T >= \boldsymbol{I}$, and $\boldsymbol{S}$ is the sphering matrix which can be determined by principal component analysis (PCA) on the matrix $(\tilde{z}(t) - < \tilde{z} >)$. After $\boldsymbol{S}$ and $\tilde{z}(t)$ have been obtained, the normalized function $h(x)$ is defined as

$$h(x) := \boldsymbol{S}(\tilde{h}(x) - < \tilde{z} >). \tag{6}$$

3) *Principal component analysis*: In order to obtain the slowest varying feature, we apply PCA to the matrix $< \dot{z}\dot{z}^T >$. The K eigenvectors with lowest eigenvalues λ_k yield the normalized weight vector w_k. w_k is defined as

$$w_k : < \dot{z}\dot{z}^T > w_k = \lambda_k w_k, \tag{7}$$

where $\lambda_1 \le \lambda_2 \le ... \le \lambda_k$. With normalized function $h(x)$ and normalized weight vector w_k, we can learn the slow feature function (i.e. the input-output function) as

$$g(t) := [g_1(t), g_2(t), ..., g_K(t)]^T, \tag{8}$$

where $g_k(t) := w_k^T h(x)$.

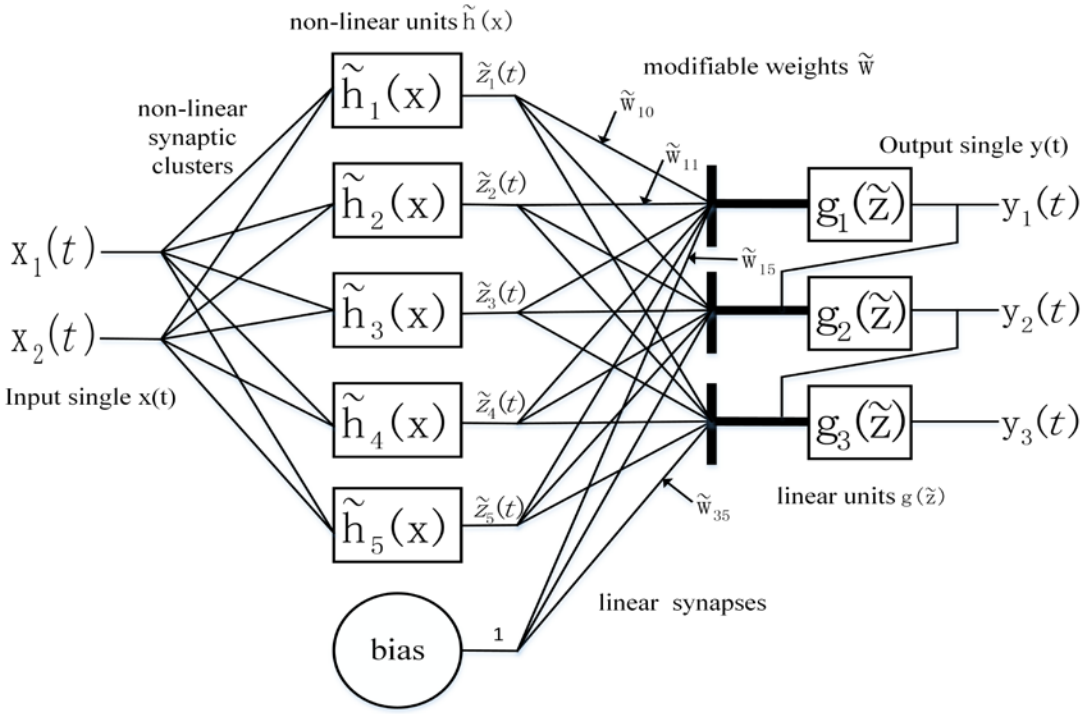

Fig. 3. The network structure for performing SFA. The components of the input signal are assumed to be normalized here.

Then, the output signal is computed instantaneously by the input-output function. The output signal $\mathrm{y}(t)$ is defined as

$$\mathrm{y}(t) \coloneqq \mathrm{g}(\mathrm{x}(t)) \tag{9}$$

where $< \mathrm{y} >= 0$, $< \mathrm{yy}^T >= \boldsymbol{I}$, and $\Delta(y_k) =< \dot{y}_k^2 >= \lambda_k$. The components of the output signal are uncorrelated, and have exactly a zero mean and unit variance. Thus, the output signal can represent the slowest varying feature and be used for sequence classification in the next step.

3.2 Learning of Slow Feature Function

Inspired by the SFA algorithm in [6], we explore two kinds of SFA learning strategies, which are the unsupervised SFA (U-SFA) and the supervised SFA (S-SFA), to extract the slow feature functions for mitosis event recognition.

1) *Unsupervised SFA*: The U-SFA learning strategy for learning the slow feature function is shown in **Fig. 4**. Based on the idea of unsupervised learning, all candidate sequences are blended together to learn the slow feature function. During the slow feature function learning process, the covariance matrix $< \mathrm{zz} >$ and the time-derivative covariance matrix $< \dot{\mathrm{z}}\dot{\mathrm{z}}^T >$ are calculated by combining all sequences together. Thus, in the U-SFA learning strategy, the unique characteristics of every mitosis cell in culture are averaged and the learned slow feature functions are shared by all candidate sequences.

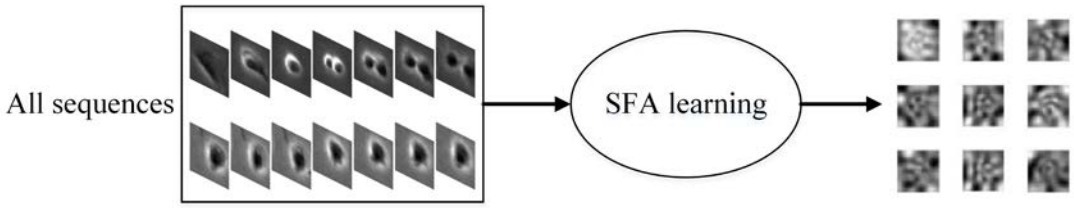

Fig. 4. The U-SFA learning strategy

2) *Supervised SFA*: The S-SFA learning strategy for learning the slow feature function is shown in **Fig. 5**. All candidate sequences are labeled as positive for containing mitosis or otherwise as negative. The S-SFA learning is performed on each category independently to extract the slow feature functions. Then, all slow feature functions are used to compute the slow feature. Apparently, the additional information given by the labels of the sequence provides more specific features for sequence classification.

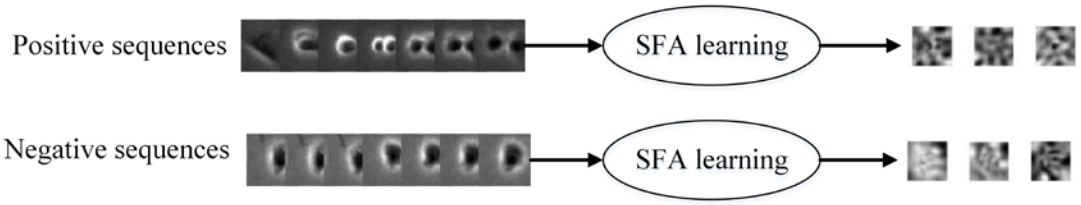

Fig. 5. The S-SFA learning strategy

After applying U-SFA and S-SFA to extract slow features from the candidate sequences, we have obtained different slow feature sequences for the subsequent sequence classification.

4. Sequence Classification Using HCRF

Hidden conditional random field (HCRF) proposed in [11] uses intermediate hidden states to model the latent structure of the input signal, and infers a single label for an input sequence, which allows us to use the training sequences that are not explicitly labeled frame-by-frame. Thus, in this paper, a HCRF model is applied to classify each candidate sequence as containing mitosis or not with the previously obtained slow feature sequences. Here we briefly review the basis of HCRF.

From HCRF we learn the mapping of the observation sequences $\mathbf{X}=\{x_1, x_2,..., x_M\}$ to the class label $y \in \mathbf{Y}$, where $x_i \in \mathbf{X}$ is a slow feature sequence proposed in the previous section. For each sequence, we also assume a vector of hidden variables $\boldsymbol{h}=\{h_1, h_2,..., h_M\}$, which is not observed in the training samples. Each $h_i \in \mathbf{H}$ captures certain underlying structure of each class and $\mathbf{H}$ is the set of hidden states in the model. The HCRF model is shown in **Fig. 6**.

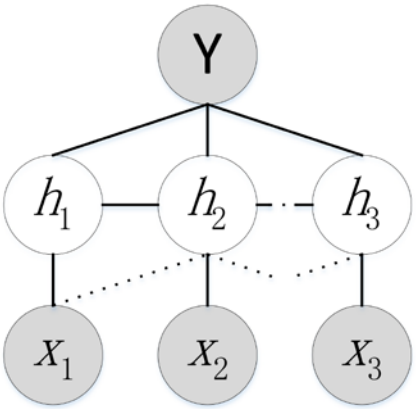

Fig. 6. The HCRF model

Given the definitions of the labels $\mathbf{Y}$, the observation sequences $\mathbf{X}$, the hidden variables $\boldsymbol{h}$, and the parameters of model $\boldsymbol{\theta}$, the HCRF computes the conditional probability of a class label given a set of observations by:

$$\mathbf{P}(y \mid \mathbf{X}, \boldsymbol{\theta}) = \sum \mathbf{P}(y, \boldsymbol{h} \mid \mathbf{X}, \boldsymbol{\theta}) = \frac{\sum_{h} e^{\Psi(y, \boldsymbol{h}, \mathbf{X}; \boldsymbol{\theta})}}{\sum_{\boldsymbol{h} \in \mathbf{H}, y' \in \mathbf{Y}} e^{\Psi(y', \boldsymbol{h}, \mathbf{X}; \boldsymbol{\theta})}}, \tag{10}$$

where $\Psi(y, \boldsymbol{h}, \mathbf{X}; \boldsymbol{\theta}) \in \mathbf{R}$ is the potential function parameterized by $\boldsymbol{\theta}$. $\Psi(y, \boldsymbol{h}, \mathbf{X}; \boldsymbol{\theta})$ is defined as

$$\Psi(y, \boldsymbol{h}, \mathbf{X}; \boldsymbol{\theta}) = \sum_{j=1}^{m} \sum_{l \in \boldsymbol{L}_1} f_{1,l}(j, y, h_j, \mathbf{X}) \boldsymbol{\theta}_{1,l} + \sum_{(j,k) \in \mathbf{E}} \sum_{l \in \boldsymbol{L}_2} f_{2,l}(j, k, y, h_j, h_k, \mathbf{X}) \boldsymbol{\theta}_{2,l}, \tag{11}$$

where $\boldsymbol{L}_1$ is the set of node features, $\boldsymbol{L}_2$ is the set of edge features, $f_{1,l}$, $f_{2,l}$ are functions which define the features in the model, and $\boldsymbol{\theta}_{1,l}$, $\boldsymbol{\theta}_{2,l}$ are the components of $\boldsymbol{\theta}$, corresponding

to the node and edge parameters. The f_1 features depend on single hidden variable values in the model, while the f_2 features depend on pairs of values.

The parameters $\boldsymbol{\theta}$ of the model can be learned from the training samples by optimizing the objective function. The objective function $\boldsymbol{L}(\boldsymbol{\theta})$ is defined as

$$\boldsymbol{L}(\boldsymbol{\theta}) = \sum_{i=1}^{N} \log \mathbf{P}(y_i \mid \mathbf{X}_i, \boldsymbol{\theta}) - \frac{1}{2\sigma^2} \|\boldsymbol{\theta}\|^2, \tag{12}$$

where N is the total number of training sequences. The first term in the objective function is the log-likelihood of the data, and the second term is the log of a Gaussian prior with the variance σ^2. For our experiments, we use the quasi-Newton gradient ascent method to search the optimal parameter values, i.e. $\boldsymbol{\theta}^* = \arg\max_{\theta} \boldsymbol{L}(\boldsymbol{\theta})$.

Given an unseen test sequence $\mathbf{X}$, the best corresponding label y^* can be computed by

$$y^* = \arg\max_{y} p(y \mid \mathbf{X}, \boldsymbol{\theta}^*). \tag{13}$$

5. Experiment

We give more detailed experimental settings and results to demonstrate the effectiveness of the SFA-based approach.

5.1 Data

The proposed classification framework was validated on the challenging phase contrast microscopy dataset named C2C12, which was acquired every 5 minutes by a Zeiss Axiovert T135V microscope (Carl Zeiss Microimaging, Thornwood, NY). The microscope is equipped with a phase contrast objective (5X, NA 0.15), a custom-stage incubator, and the InVitro software (Media Cybernetics Inc., Bethesda, MD). The C2C12 sequences contain 1013 images, and each image consists of 1393×1040 pixels of $1.3 \mu m$ / pixel.

After the acquisition of images, an expert manually annotated mitosis events in the image sequences with a labeling tool. The annotation locates the first frame of the third stage of mitosis, which contains a clearly observed boundary between two daughter cells.

5.2 Experimental results

1) Effects of different settings: To evaluate the performance with different settings in mitotic event recognition, we performed our approaches on a small part of data with different experimental settings. First, we randomly chose 1000 samples of the candidate sequences as a subset to conduct experiments. Next, we applied SFA to extract the slow feature sequences from the 1000 candidate sequences. Finally, we used a classifier for sequence classification.

The following three conditions were considered:

1. Two kinds of candidate sequences, including “image intensity” and “GIST feature”. The typical input of SFA is image intensity. For comparison, the GIST feature that represents the global image feature is also adopted.

2. Three strategies for learning slow feature functions, including “U-SFA”, “S-SFA

(positive centered)", and "S-SFA (negative centered)". For U-SFA, the input vector combines all candidate sequences to learn slow feature functions. While for S-SFA, the corresponding candidate sequences which contain or do not contain mitotic events are used to learn different slow feature functions separately.

3. Two approaches of sequence classification, including "SVM" and "HCRF". For the SVM method, the ASD feature sequences [12] are computed from the slow feature sequences, accompanied by a label. Then we use the ASD feature sequences to train the SVM model. For the HCRF method, the slow feature sequences are used to train the HCRF model directly.

We applied SVM method mainly to discover which SFA learning strategy will produce the best intrinsic dynamics between output labels. In addition, HCRF, a more powerful probabilistic model, can make full use of the temporal relations of the slow feature. In order to select the best hidden state number, which varies from 2 to 5, the ROC curve and $F1$ score ($2 \times Precision \times Recall / (Precision + Recall)$) of each hidden state number were calculated.

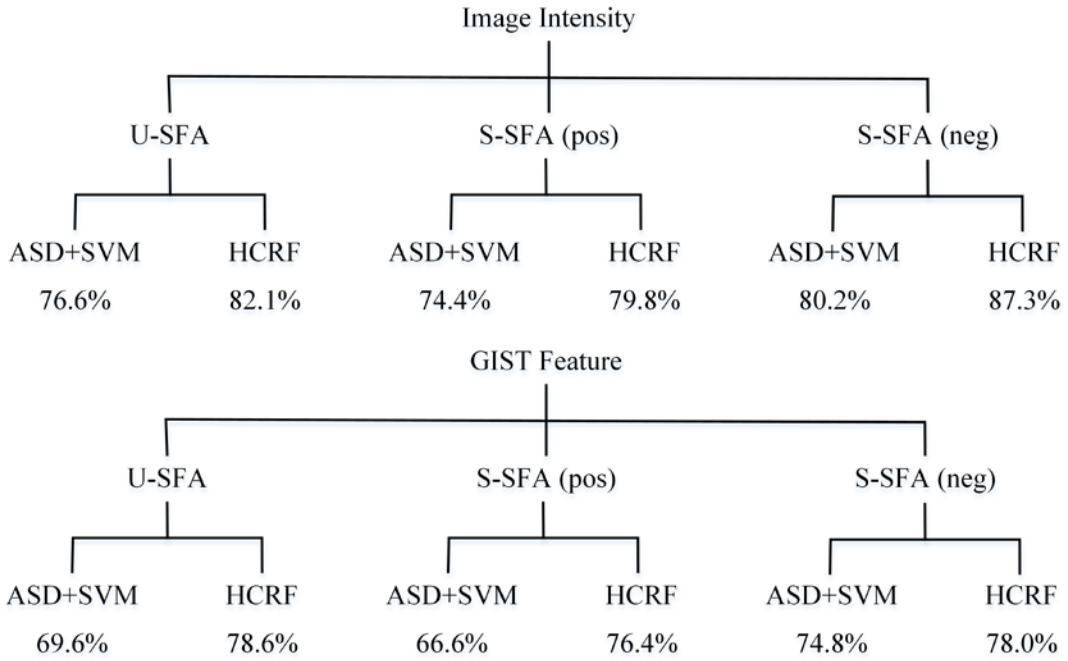

Fig. 7. The different settings and the corresponding experimental performance. One test is determined by the path from the root node to the leaf node, including data and method, and the mitosis detection accuracy is labeled under every leaf node.

Based on the performance shown in **Fig. 7**, the following conclusions can be drawn.

- By using the image intensity and GIST feature as the input signal of SFA separately, the image intensity is proven to be more effective for mitosis classification. A possible explanation is that SFA, a learning method for steady feature extraction, works more efficiently on raw data instead of extracted features.
- By using the U-SFA and S-SFA learning strategy, the performance of U-SFA is worse than that of S-SFA. This suggests that because the S-SFA strategy combines the label information of mitosis cells, the stripes in the receptive field of S-SFA are richer as shown in **Fig. 9**.

- By using the SVM and HCRF, the HCRF-based framework achieved the best performance among the proposed frameworks, because HCRF is a discriminative model that can successfully learn the hidden structure of mitosis classification problem.

After comparing the combinations mentioned above, we propose a framework in which the slow feature sequences are extracted with a S-SFA strategy, and the image intensity is fed into a HCRF classifier.

2) Performance of the proposed framework: With the effectiveness of our method proven above, we implemented the S-SFA (negative centered) strategy on the whole dataset of C2C12.

By applying the imaging-model-based microscopy image segmentation and spatiotemporal subregion extraction, we extracted candidate mitosis sequences from the input sequences. The step achieved 100% recall and a low precision. Then, the proposed combination of SFA and HCRF was used to refine the detected mitosis candidates.

For the convenience of a fair comparison, we strictly followed the split of datasets in [2], [3]. Specifically, for the C2C12 dataset, half of all mitosis events were utilized for learning and the other half for testing. To select the best hidden state number, we plotted the corresponding ROC curve of each model (shown in **Fig. 8**) and compared the area under curve (AUC) values. The best AUC of 0.93 and accuracy of 91% in C2C12 occurs at 4 hidden states.

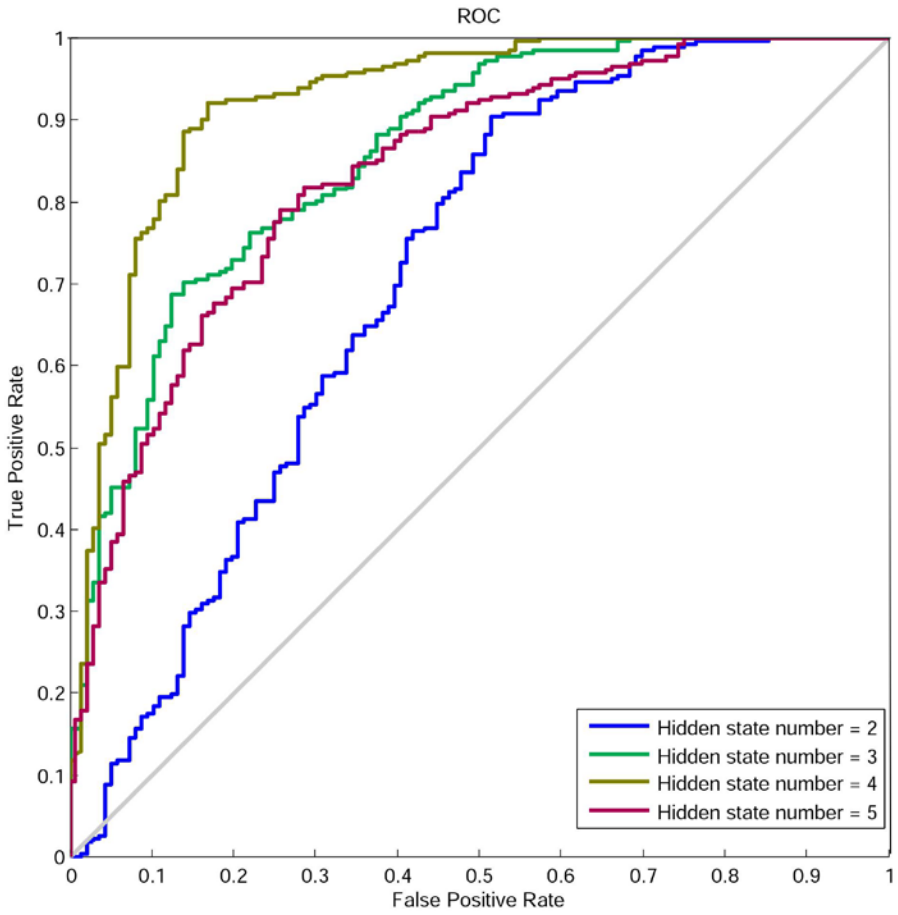

Fig. 8. The ROC curves of different hidden state numbers

We also compared the performance of our approaches with the approaches proposed in [2, 13-16] on the same dataset of C2C12. The approaches proposed in [14-16] were originally validated on another phase-contrast microscopy image dataset named C3H10T1/2, therefore we implemented the approaches and then applied them to the C2C12 dataset. The metrics we used are F1 score, precision, and recall. It can be observed from Table 1, that the proposed Image Intensity/S-SFA/HCRF approach outperforms other state-of-the-art approaches.

In the previous experiments, the HCRF classifier shows better performance than the SVM classifier. **Table 1** shows that the HCRF-based approaches (our approaches and [15]) also outperform the SVM-based framework ([13], [14], [16]). The HCRF classifier is used in our approaches and the approach proposed in [15]. However, the experimental results show that the slow feature is more suitable for current task than the combination feature of intensity histogram (IH)/histogram of oriented gradients (HoG)/GIST.

Table 1. Comparison experiments of several mitosis recognition methods

C2C12			
Method	***F1* Score**	**Precision**	**Recall**
Image Intensity/S-SFA/HCRF	**92.0%**	**93.0%**	91.0%
GIST/S-SFA/HCRF	91.8%	91.0%	**92.5%**
SIFT/EDCRF [2]	89.9%	92.4%	87.5%
LBP/SVM [13]	91.4%	93.0%	89.8%
Visual feature/SVM [14]	87.9%	86.8%	89.0%
IH, HoG, and GIST/HCRF [15]	89.6%	90.8%	88.5%
sparse representation/SVM [16]	91.2%	92.0%	90.4%

3) *The Characteristics of the learned Slow Feature Functions*: For further details of the learned slow feature functions, we chose the functions learned by U-SFA, S-SFA (positive centered), and S-SFA (negative centered).

The function g_k in (8) can be interpreted as nonlinear spatiotemporal receptive fields, and the characteristics can be confirmed with input stimuli. Assuming the *i*-th slowest signal is the *i*-th unit, each unit can have a firing rate that has no direct interpretation, which means the output is not zero when the input is zero. In our experiment, the firing rate is constrained by the zero mean constraint in (5).

Considering the convenience of analysis, we computed the optimal excitatory stimulus S^+ and the optimal inhibitory stimulus S^- for each of the three slow feature functions. S^+ denotes the input that elicits the strongest positive output, while S^- denotes the input that elicits the strongest negative output. Note that, dividing by a constant normalizes the input signal to the interval [0, 1], and S^+ and S^- can represent the typical input.

Because the label information is incorporated in the SFA learning, the stimulus of the S-SFA learning strategy has more stripes than U-SFA, which can represent more abundant information as shown in **Fig. 9**. Although the stimulus of U-SFA appears similar to that of S-SFA (pos), the stripe of S-SFA (pos) is clearer, which means the positive samples are very similar. Therefore, the slow feature sequences obtained by S-SFA (pos) do not have a good generalization performance. On the contrary, in S-SFA (neg), the generalization performance of slow feature is better because of the negative samples varies drastically. As proved in **Fig. 7,** the recognition performance of S-SFA (pos) is inferior to U-SFA, and S-SFA (neg) has the best performance.

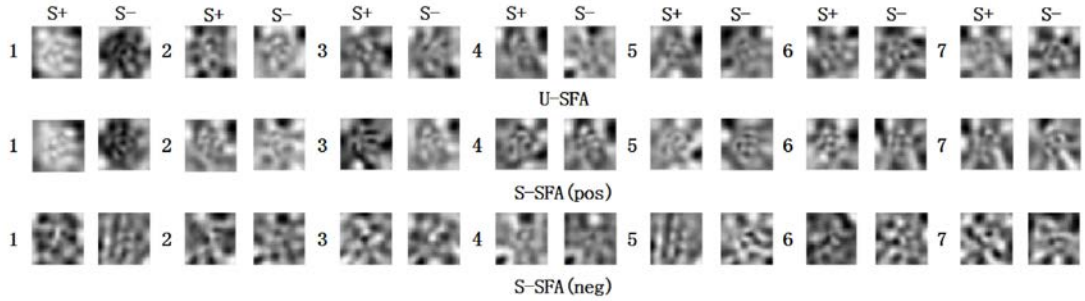

Fig. 9. Optimal stimuli in U-SFA, S-SFA (pos) and S-SFA (neg). All the blocks show the optimal excitatory stimuli (S^+) and optimal inhibitory stimuli (S^-) of the first 7 units of the simulation. S^+ contains the information about the preferred frequency and orientation of a unit, as well as the size and position of its receptive field.

For further showing how the range of the slow feature function affects the feature representation, we randomly selected 6 candidate sequences and lists the averages of the squared derivatives of the sequences after the transform step of slow feature analysis in **Fig. 10**. A greater average means that the range of the slow feature function is larger. As observed from **Fig. 10**, the slow feature function learned by the S-SFA (neg) strategy has the most drastic range, which helps to achieve the most discriminative feature representation. The observation is also proved by the results shown in **Fig. 9**. Sharing the same spirit of slow feature analysis, the negative cases have a much intense variation in cell appearance and morphology, perfectly explaining the results in **Fig. 7**.

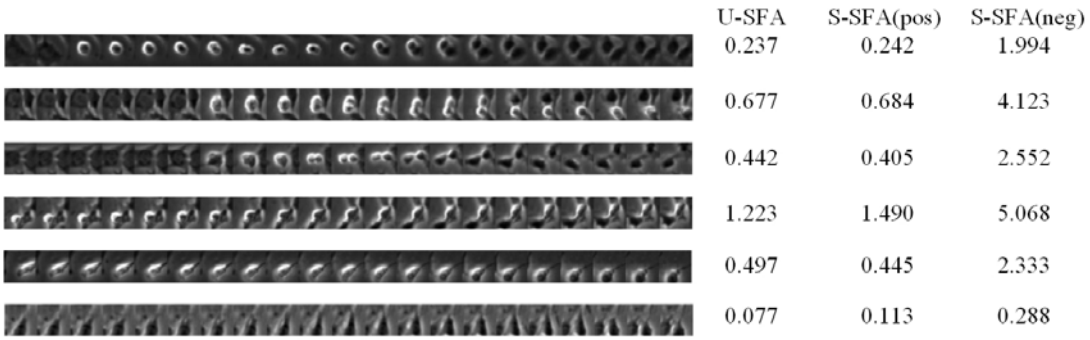

Fig. 10. The averages of squared derivatives of the candidate sequences. The left column consists of six randomly selected candidate sequences and the top three sequences contain mitotic cells.

6. Conclusion

In this paper, we present a SFA-based framework for mitotic event recognition. Algorithmically, we extend the original unsupervised SFA algorithm with three learning strategies, thus the label-related information can be encoded. We have conducted extensive experiments to evaluate the performance of the proposed method, In particular, the following conclusions can be drawn: image intensity value provides more information than GIST feature for the learning of slow feature function; the S-SFA strategy brings image content and label-related information together for better encoding; HCRF can model the temporal structure of image sequences and thus outperforms the nonsequential SVM approach; optimal

excitatory stimuli characterize the preferred frequency and orientation of a unit. In addition, the proposed method is used in not only the mitotic event recognition but also other fields of the sequence classification in computer vision. In our experiment, the proposed method achieved 0.93 area under curve (AUC) and 91% accuracy, which proves the proposed method to be a satisfactory solution for mitotic event recognition.

References

[1] K Li, ED Miller, M Chen, and T Kanade, "Computer vision tracking of stemness," in *Proc. of 5th IEEE International Symposium on Biomedical Imaging: From Nano to Macro*, pp. 847-850, May 14-17, Article (CrossRef Link).

[2] S Huh, DF Ker, R Bise, M Chen, and T Kanade, "Automated mitosis detection of stem cell populations in phase-contrast microscopy images," *IEEE Transactions on Medical Imaging*, vol. 30, no. 3, pp. 586-596, 2011. Article (CrossRef Link).

[3] AA Liu, K Li, and T Kanade, "A semi-Markov model for mitosis segmentation in time-lapse phase contrast microscopy image sequences of stem cell populations," *IEEE Transactions on Medical Imaging*, vol. 31, no. 2, pp. 359-369, 2012. Article (CrossRef Link).

[4] DG Lowe, "Distinctive Image Features from Scale-Invariant Keypoints," *International Journal of Computer Vision*, vol. 60, no. 60, pp. 91-110, 2004. Article (CrossRef Link).

[5] A Oliva, A Torralba "Chapter 2 Building the gist of a scene: the role of global image features in recognition," *Progress in Brain Research*, vol. 115, no. 2, pp. 23-36, 2006. Article (CrossRef Link).

[6] L Wiskott, TJ Sejnowski, "Slow feature analysis: unsupervised learning of invariances," *Neural Computation*, vol. 14, no. 4, pp. 715-770, 2002. Article (CrossRef Link).

[7] K Li, T Kanade, "Nonnegative Mixed-Norm Preconditioning for Microscopy Image Segmentation," *IEEE Communications Surveys and Tutorials*, in *Proc. of Information Processing in Medical Imaging: Conference*, pp. 362-373, 2009. Article (CrossRef Link).

[8] J Silvela, J Portillo, "Breadth-first search and its application to image processing problems," *IEEE Transactions on Image Processing A Publication of the IEEE Signal Processing Society*, vol. 10, no. 8, pp. 1194-1199, 2001. Article (CrossRef Link).

[9] N Ohtsu, "Unimodal thresholding," *Systems Man & Cybernetics IEEE Transactions on*, vol. 9, no. 1, pp. 62-66, 1979. Article (CrossRef Link).

[10] TTT Nguyen, G Armitage, "A survey of techniques for Internet traffic classification using machine learning," *IEEE Communications Surveys & Tutorials*, vol. 10, no. 3, pp. 56-57, 2008. Article (CrossRef Link).

[11] A Quattoni, S Wang, LP Morency, M Collins, and T Darrell, "Hidden conditional random fields," *IEEE Transactions on Pattern Analysis & Machine Intelligence*, vol. 29, no. 10, pp. 1848-1853, 2007. Article (CrossRef Link).

[12] Z Zhang, D Tao, "Slow feature analysis for human action recognition," *IEEE Transactions on Software Engineering*, vol. 34, no. 3, pp. 436-450, 2012. Article (CrossRef Link).

[13] S Huh, FEK Dai, H Su, and T Kanade, "Apoptosis Detection for Adherent Cell Populations in Time-Lapse Phase-Contrast Microscopy Images," in *Proc. of Medical Image Computing & Computer-assisted Intervention: Miccai International Conference on Medical Image Computing & Computer-assisted Intervention*, pp. 331-339, 2012. Article (CrossRef Link).

[14] A Liu, K Li, T Kanade, "Spatiotemporal mitosis event detection in time-lapse phase contrast microscopy image sequences," in *Proc. of IEEE International Conference on Multimedia and Expo*, pp. 19-23, 2010. Article (CrossRef Link).

[15] A Liu, K Li, T Kanade, "Mitosis sequence detection using hidden conditional random fields," in *Proc. of IEEE International Symposium on Biomedical Imaging: From Nano to Macro*, pp. 580-583, 2010. Article (CrossRef Link).

[16] A Liu, T Hao, Z Gao, Y Su, Z Yang, "Nonnegative Mixed-Norm Convex Optimization for Mitotic Cell Detection in Phase Contrast Microscopy," *Computational & Mathematical Methods in Medicine*, vol. 2013, no. 4, pp. 491-497, 2013. Article (CrossRef Link).

Jinghui Chu received the B.Eng. degree in radio technology, and M.Eng. and Ph.D. degrees in signal and information processing all from Tianjin University, Tianjin, China, in 1991, 1997, and 2006 respectively. She is currently an associate professor in the School of Electronic Information Engineering, Tianjin University. Her teaching and research interests include digital video technology and pattern recognition.

Hailan Liang received her B.E degree in electronic information engineering from Tianjin University, Tianjin, P.R. China, in June 2014. She is currently pursuing a master's degree at the School of Electronic Information Engineering in Tianjin University. Her current research interests include machine learning and image processing.

Zheng Tong received his B.E degree in electronic information engineering from Zhejiang Normal University, Zhejiang, P.R. China, in June 2014.
He is currently pursuing a master's degree at the School of Electronic Information Engineering in Tianjin University. His current research interests include pattern recognition and machine learning.

Wei Lu received his B.Eng. degree in Electronic Engineering, and Ph.D. degree in signal and information processing from Tianjin University, Tianjin, China, in 1998 and 2003, respectively. He is currently an associate professor in the School of Electronic Information Engineering, Tianjin University. His teaching and research interests include digital filter design, digital multimedia technology, embedded system design, Web application design, and pattern recognition. He is now a senior member of the Chinese Institute of Electronics